Cerebral Metabolic Alterations in Rats With Diabetic Ketoacidosis

Effects of Treatment With Insulin and Intravenous Fluids and Effects of Bumetanide

Nicole Glaser,[1] Natalie Yuen,[2] Steven E. Anderson,[2] Daniel J. Tancredi,[1] and Martha E. O'Donnell[2]

OBJECTIVE—Cerebral edema is a life-threatening complication of diabetic ketoacidosis (DKA) in children. Recent data suggest that cerebral hypoperfusion and activation of cerebral ion transporters may be involved, but data describing cerebral metabolic alterations during DKA are lacking.

RESEARCH DESIGN AND METHODS—We evaluated 50 juvenile rats with DKA and 21 normal control rats using proton and phosphorus magnetic resonance spectroscopy (MRS). MRS measured cerebral intracellular pH and ratios of metabolites including ATP/inorganic phosphate (Pi), phosphocreatine (PCr)/Pi, N-acetyl aspartate (NAA)/creatine (Cr), and lactate/Cr before and during DKA treatment. We determined the effects of treatment with insulin and intravenous saline with or without bumetanide, an inhibitor of Na-K-2Cl cotransport, using ANCOVA with a 2 × 2 factorial study design.

RESULTS—Cerebral intracellular pH was decreased during DKA compared with control (mean ± SE difference −0.13 ± 0.03; $P < 0.001$), and lactate/Cr was elevated (0.09 ± 0.02; $P < 0.001$). DKA rats had lower ATP/Pi and NAA/Cr (−0.32 ± 0.10, $P = 0.003$, and −0.14 ± 0.04, $P < 0.001$, respectively) compared with controls, but PCr/Pi was not significantly decreased. During 2-h treatment with insulin/saline, ATP/Pi, PCr/Pi, and NAA/Cr declined significantly despite an increase in intracellular pH. Bumetanide treatment increased ATP/Pi and PCr/Pi and ameliorated the declines in these values with insulin/saline treatment.

CONCLUSIONS—These data demonstrate that cerebral metabolism is significantly compromised during DKA and that further deterioration occurs during early DKA treatment—consistent with possible effects of cerebral hypoperfusion and reperfusion injury. Treatment with bumetanide may help diminish the adverse effects of initial treatment with insulin/saline. ***Diabetes*** **59:702–709, 2010**

From the [1]Department of Pediatrics, University of California, Davis, California; and the [2]Department of Physiology and Membrane Biology, University of California, Davis, California.

Corresponding author: Nicole Glaser, nsglaser@ucdavis.edu.

Received 29 April 2009 and accepted 9 December 2009. Published ahead of print at http://diabetes.diabetesjournals.org on 22 December 2009. DOI: 10.2337/db09-0635.

Cerebral injury resulting from diabetic ketoacidosis (DKA) is the most frequent diabetes-related cause of death in children. The cause of this complication has been a subject of much debate and is not well understood. Recent data from studies using an animal model demonstrate that DKA is associated with reduced cerebral blood flow and with brain cell swelling (1,2). The same studies suggest that activation of cerebral microvascular endothelial ion transport (particularly Na-K-Cl cotransport) during DKA contributes to brain cell swelling in this setting, as it does in animal models of stroke. During DKA treatment with insulin and intravenous fluids, cerebral blood flow rises and vasogenic edema develops (3,4). These data suggest that cerebral injury resulting from DKA may be similar to hypoxic/ischemic brain injury resulting from stroke or other causes and raise the question of whether bumetanide, an inhibitor of Na-K-Cl cotransport, may be helpful in reducing cerebral injury in the setting of DKA.

Children who develop DKA-related cerebral injury often present with normal mental status or only mild mental status abnormalities. After several hours of DKA treatment, however, these patients have a decline in mental status often followed by loss of consciousness and sometimes by clinical signs of increased intracranial pressure. Although a small percentage of children have clinically apparent cerebral injury at presentation of DKA prior to treatment, neurological decline during DKA treatment is more common (5–7). Why children may worsen during treatment with insulin and intravenous fluids is not clear. Initial hypotheses focused on the role of fluid infusion and osmotic change in brain cell swelling (8,9). More recent data suggest instead that reperfusion injury or related mechanisms may be more likely (1–3).

Magnetic resonance spectroscopy (MRS) provides a noninvasive method for evaluating cerebral metabolism. Proton MRS can be used to measure concentrations of lactate in the brain, as well as the relative concentrations of N-acetyl aspartate (NAA) and creatine (Cr), a measure thought to be indicative of neuronal health (10,11). In stroke and other forms of hypoxic/ischemic brain injury, brain lactate is elevated and NAA/Cr is reduced. Phosphorus MRS can be used to measure cerebral intracellular pH and concentrations of high-energy phosphates, which typically decrease during hypoxia/ischemia (12–15).

MRS provides an ideal method to evaluate the cerebral metabolic alterations associated with DKA and the changes in cerebral metabolic state that occur during DKA

treatment with insulin and intravenous fluids. We undertook the current study to characterize these metabolic changes and to determine the effects of treatment with bumetanide, an inhibitor of Na-K-2Cl cotransport in the blood-brain barrier (BBB) and astrocytes, as well as many other cell types, on these metabolic alterations. In analogy with ischemia/reperfusion injury, we hypothesized that DKA would be associated with metabolic abnormalities similar to those of hypoxic/ischemic brain injury and that these abnormalities would worsen during initial DKA treatment as normal cerebral perfusion is reestablished. Further, we hypothesized that bumetanide treatment would result in improvements in the cerebral metabolic state.

RESEARCH DESIGN AND METHODS

A sequence of two experiments was performed. The first experiment compared metabolic measures in 50 rats with DKA to 21 normal control rats. DKA rats were then randomized to one of the four treatment combinations from a 2×2 factorial experiment designed to assess the treatment effects of insulin/saline and bumetanide. Twelve rats were treated with bumetanide only, 11 with insulin/saline only, 14 with both and 13 DKA control rats were treated with neither. To assess whether estimates of the bumetanide-only effect could be confounded with the small volume of saline fluid used to deliver bumetanide intravenously, five of the 13 DKA control rats were intentionally treated with a small volume of saline and compared with the remaining control rats.

Induction of DKA. Seventy-one 4-week-old Sprague-Dawley rats (150 g; Charles River Laboratories, Wilmington, MA) were given an intraperitoneal injection of streptozotocin (STZ) (150 mg/kg; $n = 50$) or STZ vehicle as previously described (1). Rats were given unlimited access to D10W (water with 10% dextrose; Fisher Scientific, Santa Clara, CA) in the first 24-h period after STZ injection to prevent hypoglycemia and then were subsequently allowed unlimited access to tap water and standard rat chow. Rats were weighed daily. Urine glucose and ketoacids (acetoacetate) were measured using Multistix urinalysis strips (Fisher Scientific; Bayer) as previously described (1). Rats in the DKA group had urine glucose and acetoacetate concentrations $\geq$110 mmol/l and $\geq$15,680 μmol/l, respectively. To induce a level of dehydration similar to severe human DKA and to ensure acidosis, we deprived rats of drinking water 24 h before imaging. This study was conducted in accordance with the Animal Use and Care Guidelines issued by the National Institutes of Health using a protocol approved by the Animal Use and Care Committee at the University of California, Davis.

Magnetic resonance imaging. MRS measurements were performed in anesthetized rats in a horizontal bore magnet (Oxford Instruments, Oxford, U.K.) using a two-channel Biospec system (Bruker Biospin, Billerica, MA) running ParaVision software. A double-tuned 1H/X Litz coil (Doty Scientific, Columbia, SC) was used, where X is tunable for ^{23}Na or ^{31}P. Field homogeneity was optimized by localized shimming on ^{1}H over a $9 \times 9 \times 9$ mm voxel of interest (VOI). The VOI was positioned inside the brain and selected to encompass as much of the cortex as possible. After shimming, ^{31}P- and ^{1}H-MRS data were acquired.

^{31}P-MRS. An $8 \times 8 \times 8$ mm VOI was centered on the shimmed volume. Spectra were acquired in 43.2-min intervals using Bruker software for image-selected in vivo spectroscopy, (repetition time [TR] 4 s, 80 signals averaged, and 26-Hz line broadening). Intracellular pH was calculated from the chemical shift of the inorganic phosphate (Pi) peak relative to the phosphocreatine (PCr) peak using the equation $pH_i = 6.7 + \log [(\text{shift} - 3.186)/(5.691 - \text{shift})]$ (16). PCr, β-ATP, and Pi peaks were integrated using NUTS software (Acorn NMR, Livermore, CA) and presented as ratios (ATP to Pi and PCr to Pi).

^{1}H-MRS. A $7 \times 7 \times 7$ mm VOI was centered on the shimmed volume. Acquisition of ^{1}H-MRS data was initiated immediately after ^{31}P-MRS acquisition was completed. Spectra were collected in 2.8-min intervals, but to improve the signal-to-noise ratio for ^{1}H measurements, two 2.8-min files were added together for final analysis. Data were acquired using Bruker software for point-resolved spectroscopy (TR 6,974 ms, 20 signals averaged, and 2-Hz line broadening) with chemical shift–selective pulses and dephasing gradients to suppress water. Cerebral ^{1}H metabolite peaks were identified according to their chemical shifts (17): NAA 2.02 ppm, Cr 3.0 ppm, lactate 1.38 ppm, and β-hydroxy butyrate (βOHB) 1.15 ppm. With an echo time (TE) of 132 ms, the lipid peak was suppressed, and the lactate and βOHB appeared as inverted peaks. The NAA, Cr, lactate, and βOHB peaks were integrated using NUTS software and presented as ratios (NAA to Cr, lactate to Cr, and βOHB to Cr).

Experimental treatments: saline and insulin infusion. For treatment with saline and insulin, rats were infused via cannulated femoral vein with regular insulin at 1.5 units $\cdot$ kg^{-1} $\cdot$ h^{-1} (Humulin; Lilly & Company, Indianapolis, IN) and 0.9% NaCl at 80 ml $\cdot$ kg^{-1} $\cdot$ h^{-1} for 1 h, followed by infusion with insulin and saline at 1.5 units $\cdot$ kg^{-1} $\cdot$ h^{-1} and 40 ml $\cdot$ kg^{-1} $\cdot$ h^{-1}, respectively, for the remainder of the 2-h experiment. These rates were determined by comparisons of human versus rat metabolic rate, body surface area, and percentage dehydration during DKA. In initial studies, these rates of infusion resulted in biochemical changes during DKA treatment (decline in serum glucose and urea nitrogen concentrations and resolution of acidosis) at rates similar to those observed in children with DKA.

Bumetanide treatments. For experiments designed to evaluate the effects of bumetanide on cerebral metabolite concentrations, bumetanide (30 mg/kg) was administered in one of two ways. For rats not receiving intravenous infusion of saline and insulin, bumetanide was injected into a femoral vein cannula (0.8 cc total volume) immediately before the start of imaging, as previously described (1). For rats treated with saline and insulin infusion, bumetanide was given via femoral vein cannula at the start of the saline and insulin infusion. Bumetanide (ICN Biomedicals, Costa Mesa, CA) was prepared as previously described (1).

Animal preparation for imaging. Prior to imaging, rats were anesthetized using Na pentobarbital (65 mg/kg i.p.). Body temperature was monitored via rectal probe (Cole-Parmer Instruments, Vernon Hills, IL), and a heating pad with circulating water (Gaymar Inc., Orchard Park, NY) maintained body temperature at 36.8–37.0°C throughout surgery and brain imaging. The femoral artery and vein were cannulated for blood sampling and for drug and treatment infusion, respectively. Rats were subjected to tracheal intubation and ventilated (Harvard Small Animal Ventilator, Holliston, MA) throughout surgery and imaging. Ventilation was done to offset the tendency toward respiratory depression in the anesthetized rats and thereby ensure that the animal model closely mimicked human DKA. Blood samples were analyzed for pCO_2 and pH immediately after intubation and the respiratory rate and tidal volume adjusted with the goal of maintaining pCO_2 levels within the range expected for a normal physiological response to the degree of acidosis (18).

Blood chemistry. Blood samples were withdrawn from the femoral artery cannula, before and hourly during imaging, and from the abdominal aorta, after imaging, at the conclusion of the experiment. We measured serum electrolyte concentrations, pH, blood urea nitrogen, and glucose concentrations using an I-STAT portable clinical analyzer (Sensor Devices, Waukesha, WI).

Statistical analysis. All statistical analyses were conducted using version 9.1 of the SAS system for Windows. Two-sided testing was used for all study hypotheses, with P values <0.05 considered statistically significant and between 0.05 and 0.10 considered representative of a trend.

Statistical analysis began with graphical and numerical summaries of the distributions of study outcomes and baseline measurements. When indicated, variables were log transformed to ameliorate skewness or to stabilize variances across the groups under comparison. Group-specific (geometric) means and (geometric) SDs are reported for (log-transformed) baseline measures. At baseline, biochemical measures for some rats fell above or below the detection limits of measurement (blood urea nitrogen, log-transformed TCO_2, and serum glucose concentrations). To account for this, maximum likelihood estimates of pretreatment distribution parameters for these measures were produced, with normal distributions assumed.

For comparing DKA rats with normal control rats, Student's independent-groups t test was used for all outcomes except those with some values outside the detection limits of measurement, which were analyzed using maximum-likelihood estimates of regression models for heterogeneous, limited, dependent, and normally distributed variables (using SAS PROC QLIM). These models used a single independent variable that indicated group membership (one "DKA rat" versus zero "control rat"). The coefficient for this regressor was compared with the heterogeneity-robust SE estimate to form the t statistic used for testing between-group differences.

Student's t test was used within the set of DKA control rats to compare the eight untreated rats with the five administered a small amount of saline. These comparisons were performed on baseline values and on change scores (from pre- to posttreatment). After establishing that these two subgroups did not have statistically significant differences on any comparison, the two subgroups were analyzed as a single group in subsequent analyses.

Within each of the four factorial treatment combinations, over-time changes in metabolite ratios were assessed using paired t tests comparing pre- and posttreatment values. Between-group comparisons on over-time changes were conducted using ANCOVA models for a 2×2 factorial experiment, with main effects for the two binary treatment factors and, when indicated, heterogeneous error variance components. Baseline covariates were selected based on a preliminary stage of analysis that aimed to find a parsimonious set of predictors to improve model fit and the precision of estimates of main treatment effects. This set included serum pH for all study outcomes and, for

TABLE 1
Biochemical values in normal control rats and in rats with DKA before and after 2-h treatment with insulin and saline infusion

	Control	DKA before infusion	DKA after 2-h saline and insulin infusion
n	21	49	11
Glucose (mmol/l)	7.9 ± 0.9	35.7 ± 9.1	17.3 ± 8.4
BUN (mmol/l	3.9 ± 1.1	34.3 ± 13.2	25.3 ± 10.7
pH	7.42 ± 0.06	7.10 ± 0.23	7.20 ± 0.13
Total CO_2 (mmol/l	27 ± 1	7 ± 2	12 ± 1

Data are means ± SD for glucose, BUN, and pH and geometric means ± SD for total CO_2. DKA preinfusion values represent pooled values for all DKA treatment groups. Postinfusion values include rats in the standard (insulin and saline) DKA treatment group only. Among DKA rats before infusion, 20 of 49 had glucose measurements above the detection limit of 38.5 mmol/l, 9 of 49 had BUN measurements above the detection limit of 50 mmol/l, and 18 of 48 had a total CO_2 measurement below the detection limit of 5 mmol/l. Pretreatment parameters for BUN, glucose, and total CO_2 are maximum-likelihood estimates, as described in RESEARCH DESIGN AND METHODS.

outcomes where it improved model fit, an indicator for whether the baseline value of TCO_2 was outside the limit of detection. PCO_2 was also evaluated as a candidate variable for inclusion in the model but was not found to improve model fit. Between-model comparisons for goodness of fit were performed using the Akaike information criterion and by comparing the root mean square error of the residuals. Analysis of residuals and influence statistics and fits of alternative regression models (with interaction terms) were used to verify that models for mean and covariance parameters were appropriately specified, were not unduly influenced by a small number of extreme observations, and satisfied distributional assumptions needed for valid hypothesis testing. To accommodate the features of our final model, we used PROC MIXED to estimate model parameters using restricted maximum-likelihood estimates for variance components.

RESULTS

Biochemical values for DKA and normal control rats are summarized in Table 1. Using phosphorus MRS, we found that rats with DKA had significantly decreased cerebral intracellular pH compared with that in normal control rats (Fig. 1). Peaks corresponding to the ketone body, βOHB, were readily detectable on proton MRS in DKA rats (mean βOHB-to-Cr ratio −0.16 ± 0.12), whereas no such peaks could be identified in normal control rats. Lactate-to-Cr ratios were significantly increased on proton MRS in DKA rats, and NAA-to-Cr ratios were significantly decreased compared with control values. In phosphorus MRS, ATP-to-Pi ratios were significantly decreased in DKA rats compared with those in normal controls, but PCr-to-Pi ratios were not significantly different between the two groups.

When rats with DKA were treated with intravenous insulin and saline, a deterioration in MRS measures of cerebral metabolism occurred (Figs. 2 and 3). We observed a significant decrease in ATP-to-Pi, PCr-to-Pi, and NAA-to-Cr ratios in rats treated with insulin and saline for 2 h (Fig. 4*A*–*C*). These changes occurred despite improvements in cerebral intracellular pH (Fig. 4*D*) and decreased brain levels of βOHB (cerebral βOHB-to-Cr 0.12 ± 0.07 before treatment vs. 0.03 ± 0.03 after treatment; $P < 0.001$), consistent with improvements in the ketoacidotic state. In contrast, rats with DKA who were left untreated for the same 2-h period had no significant changes in ATP-to-Pi, PCr-to-Pi, and NAA-to-Cr ratios, cerebral intra-

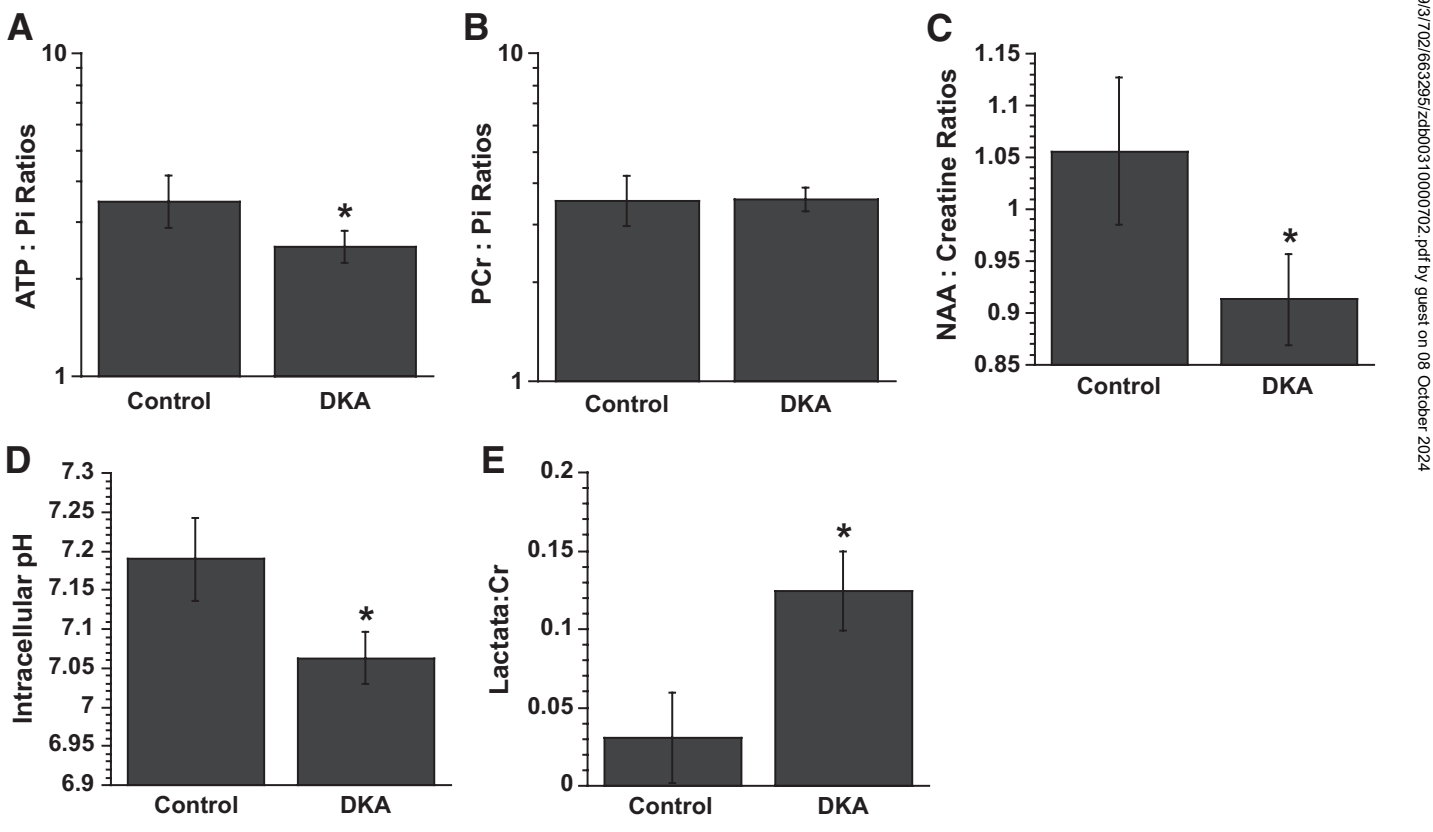

FIG. 1. Cerebral metabolites measured by ^{1}H- and ^{31}P-MRS in DKA and control rats. *A*: ATP-to-Pi ratios. *B*: PCr-to-Pi ratios. *C*: NAA-to-Cr ratios. *D*: Intracellular pH. *E*: Lactate-to-Cr ratios. All values are means (95% CI). *A* and *B* are geometric means; *C*, *D*, and *E* are arithmetic means. n = 20 for control and 41 for DKA rats in *C* and *D*; n = 20 for control and 44 for DKA rats in *A*, *B*, and *E*. *Values are significantly different from those of the control group; P values <0.005.

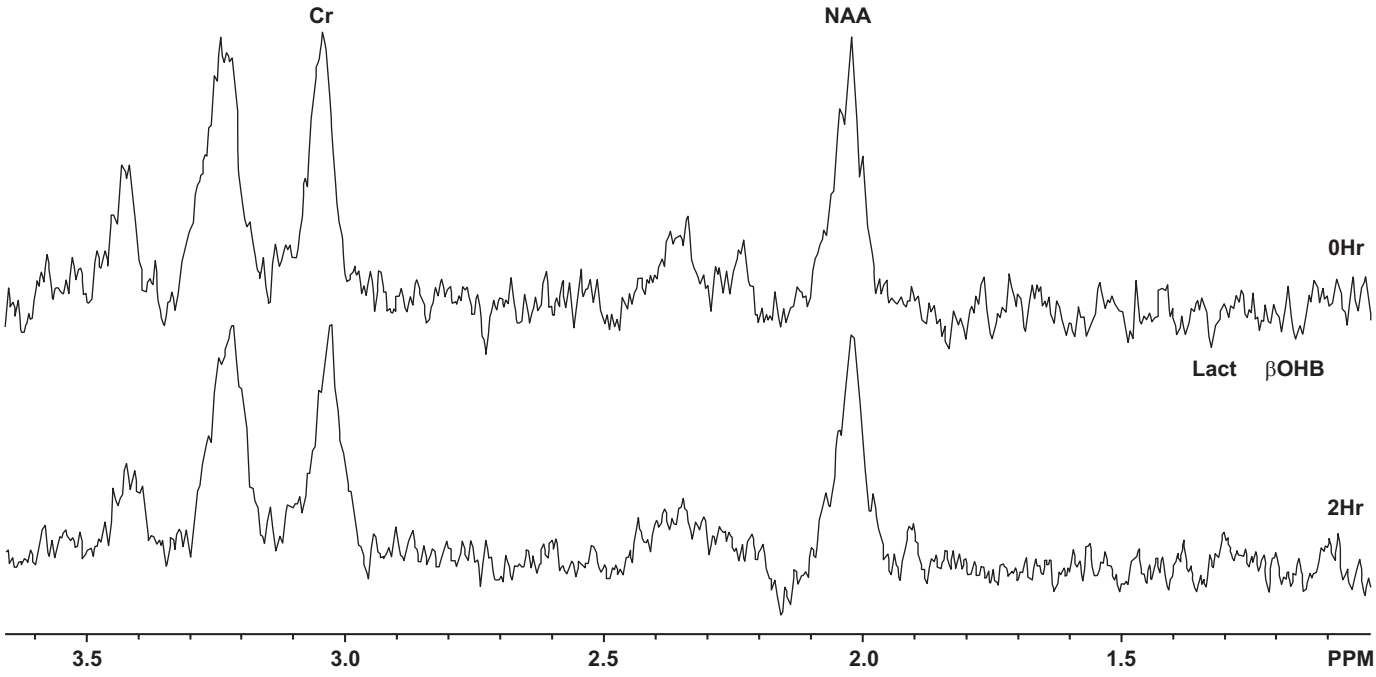

FIG. 2. ^{1}H-MR spectra obtained before DKA treatment and at the end of 2-h treatment with insulin and saline. Lact, lactate.

cellular pH (Fig. 4*A*–*D*), or intracerebral βOHB-to-Cr ratio (0.17 ± 0.06 vs. 0.18 ± 0.11; $P = 0.84$).

When bumetanide was added to the insulin and saline treatment, the mean ATP-to-Pi, PCr-to-Pi, and NAA-to-Cr ratios showed no significant change during treatment rather than declining (Fig. 4*A*–*C*). Treatment of DKA rats with bumetanide alone, without insulin or saline, resulted in improvements in some metabolic measures. ATP-to-Pi ratio rose significantly, and there was a trend toward an increase in PCr-to-Pi ratio ($P = 0.051$). NAA-to-Cr levels, however, did not improve significantly in this group, and intracellular pH did not either (Fig. 4*D*). Results of the ANCOVA analysis (Table 2) confirmed significant opposing effects of insulin and saline versus bumetanide. While insulin and saline treatment worsened MRS metabolic measures despite improvements in intracellular pH, bumetanide treatment tended to improve MRS metabolic measures without significantly changing intracellular pH.

DISCUSSION

Case reports of cerebral edema and cerebral injury occurring during DKA in children often describe the child's initial mental state as normal or nearly normal at the time

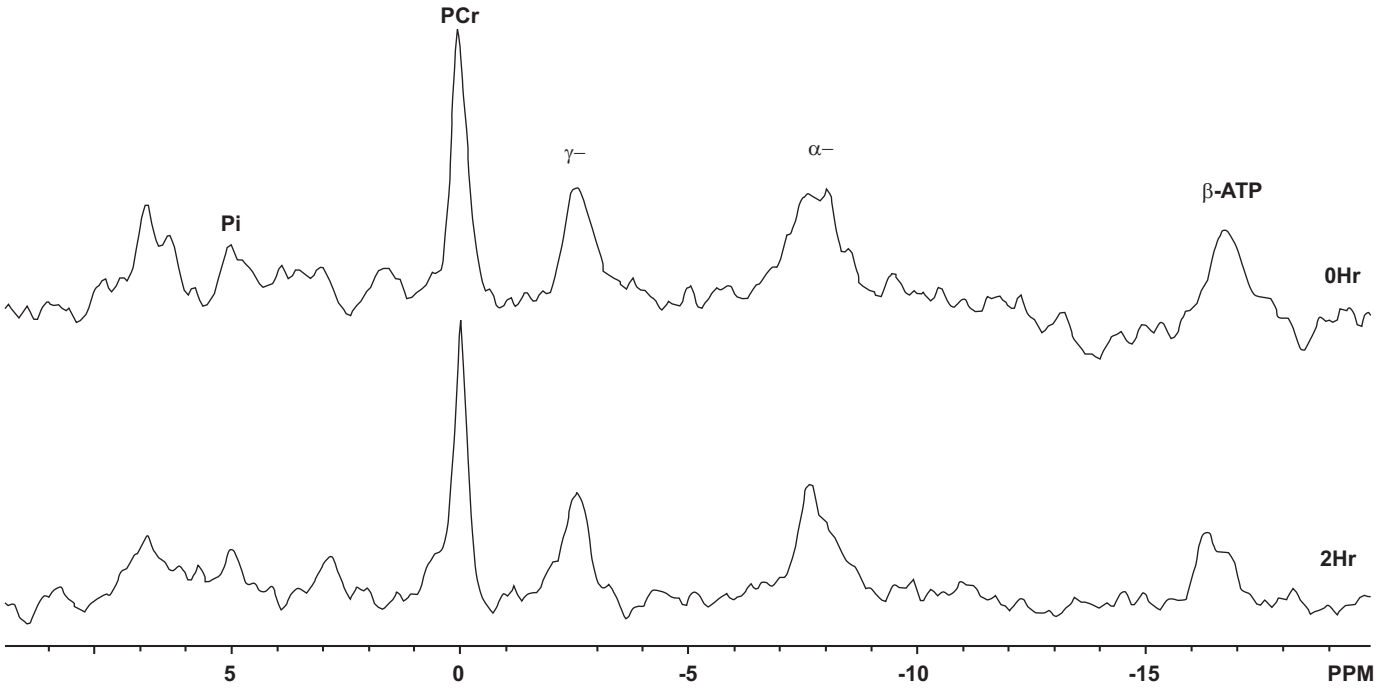

FIG. 3. ^{31}P-MR spectra obtained before DKA treatment and at the end of 2-h treatment with insulin and saline. α–, αATP; γ–, γATP.

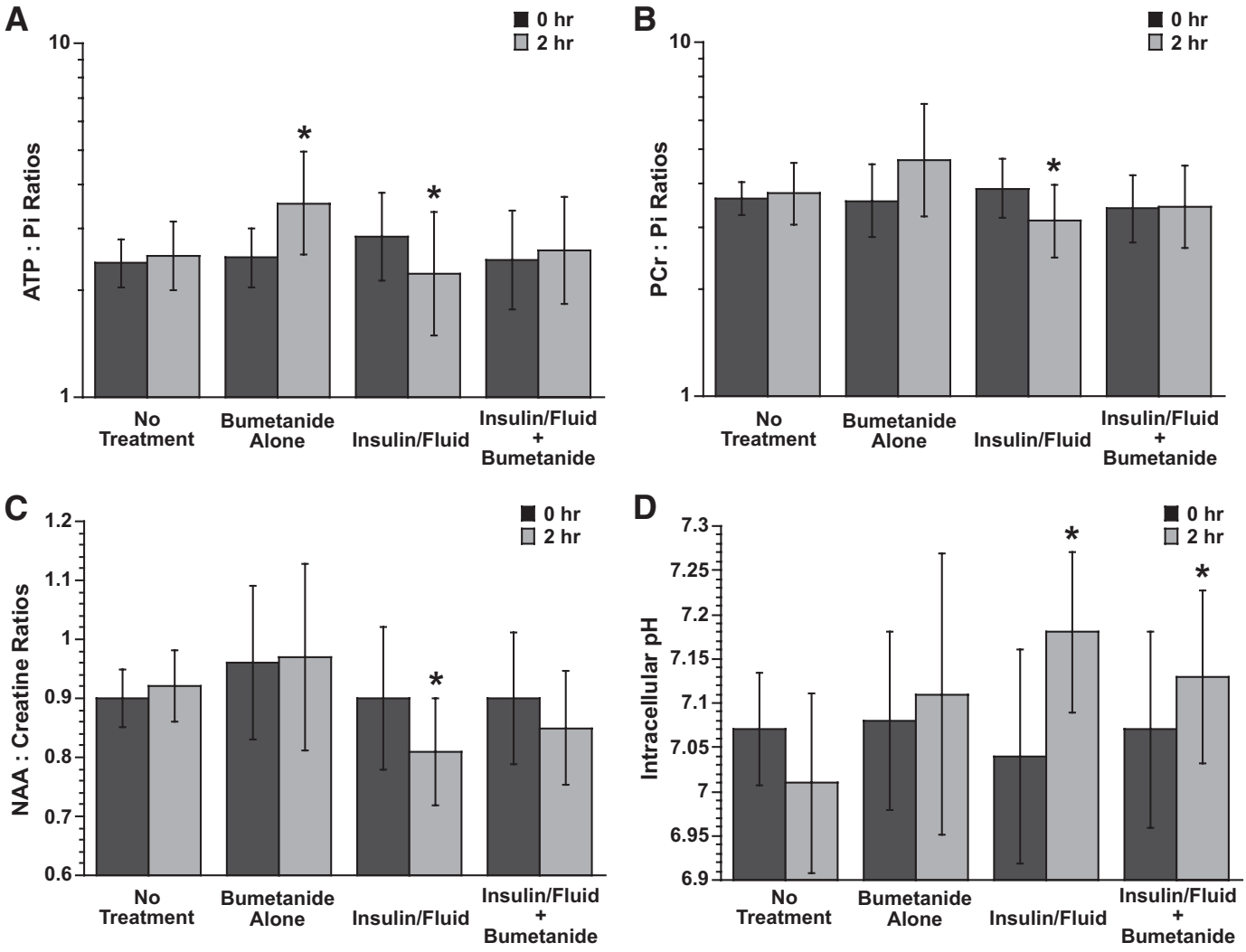

FIG. 4. *A*: ATP-to-Pi ratios in DKA rats before and after saline and insulin infusion with and without bumetanide. ATP-to-Pi ratios were measured by ^{31}P-MRS as described in RESEARCH DESIGN AND METHODS. Bumetanide alone and saline plus insulin with and without bumetanide treatments were started immediately after baseline measurements (0 h). All values are geometric means (95% CI); n = 12, 10, 10, and 12 for no treatment, bumetanide alone, saline and insulin, and saline and insulin with bumetanide treatment groups, respectively. *Within-group comparisons: P < 0.02 for comparison of pre-/posttreatment values in the bumetanide-alone group and the insulin-and-fluid group. Refer to Table 2 for the overall effects of insulin plus saline and bumetanide. Data were analyzed with log-transformed values. *B*: PCr-to-Pi ratios in DKA rats before and after saline and insulin infusion with and without bumetanide. PCr-to-Pi ratios were measured by ^{31}P-MRS as described in RESEARCH DESIGN AND METHODS. Bumetanide alone and saline and insulin with and without bumetanide treatments were started immediately after baseline measurements (0 h). All values are geometric means (95% CI); n = 12, 10, 10, and 12 for no treatment, bumetanide alone, saline and insulin, and saline and insulin with bumetanide treatment groups, respectively. *Within-group comparisons: P = 0.01 for comparison of pre- and posttreatment values in the insulin-and-fluid group. P = 0.051 for comparison of pre- and posttreatment values in the bumetanide-alone group. Refer to Table 2 for the overall effects of insulin plus saline and bumetanide. Data were analyzed with log-transformed values. *C*: NAA-to-Cr ratios in DKA rats before and after saline and insulin infusion with and without bumetanide. NAA-to-Cr ratios were measured by ^{1}H-MRS as described in RESEARCH DESIGN AND METHODS. Bumetanide alone and saline and insulin with and without bumetanide treatments started immediately after baseline measurements (0 h). All values are arithmetic means (95% CI); n = 13, 9, 9, and 10 for no treatment, bumetanide alone, saline and insulin, and saline and insulin with bumetanide treatment groups, respectively. *Within-group comparisons: P = 0.03 for comparison of pre- and posttreatment values in the insulin-and-fluid group. Refer to Table 2 for the overall effects of insulin plus saline and bumetanide. *D*: Intracellular pH in DKA rats before and after saline and insulin infusion with and without bumetanide. Intracellular pH values were determined by ^{31}P-MRS as described in RESEARCH DESIGN AND METHODS. Bumetanide alone and saline and insulin with and without bumetanide treatments were started immediately after baseline measurements (0 h). All values are arithmetic means (95% CI); n = 12, 10, 10, and 12 for no treatment, bumetanide alone, saline and insulin, and saline and insulin with bumetanide treatment groups, respectively. *Within-group comparisons: P < 0.05 for comparison of pre- and posttreatment values in the insulin-and-fluid group and the insulin-and-fluid plus bumetanide group. Refer to Table 2 for the overall effects of insulin plus saline and bumetanide.

of presentation with DKA. After several hours of treatment with insulin and intravenous fluids, however, a decline in mental status occurs, often with loss of consciousness, seizures, or other substantial neurological abnormalities (19–21). This decline in mental status occurs despite improvements in acidosis and hyperglycemia. Although clinically apparent cerebral edema and cerebral injury can also occur before treatment of DKA, the more frequent occurrence of cerebral edema during DKA treatment suggests that some aspect of treatment may cause or enhance cerebral injury.

Our data demonstrate that cerebral intracellular pH is low during untreated DKA, cerebral lactate levels are high, and levels of high-energy phosphates are low, similar to cerebral ischemia. NAA-to-Cr ratios are also decreased, suggesting neuronal compromise or injury (10–14,22–25). Taken together with our previous results demonstrating that DKA diminishes cerebral blood flow in this model (2),

TABLE 2
Individual effects of insulin and saline with bumetanide on cerebral metabolites during DKA: regression-adjusted main effects of each treatment

Metabolite	Adjusted main effect of insulin and saline	*P*	Adjusted main effect of bumetanide	*P*
ATP-to-Pi	−0.34 ± 0.13	0.02	0.38 ± 0.15	0.01
PCR-to-Pi	−0.29 ± 0.10	0.007	0.31 ± 0.13	0.03
NAA-to-Cr	−0.08 ± 0.03	0.020	−0.001 ± 0.03	0.97
Intracellular pH	0.13 ± 0.04	0.005	−0.002 ± 0.04	0.72

Data are means ± SE unless otherwise indicated. ATP-to-Pi and PCR-to-Pi ratios were analyzed as log-transformed values.

these data provide further evidence consistent with the hypothesis that cerebral hypoperfusion occurs in untreated DKA and may lead to cerebral injury. Similar findings have been observed in both human and animal studies of stroke and other ischemic brain injury, including declines in brain concentrations of high-energy phosphates, elevated brain lactate concentrations, and decreased NAA-to-Cr ratios (12,14,15,23–26). Additionally, our data provide the first evidence that during initial DKA treatment with insulin and intravenous saline, key aspects of the cerebral metabolic state worsen. High-energy phosphate levels decline further, as does the NAA/Cr ratio. These data suggest that the initial period of DKA treatment may lead to additional cerebral injury possibly caused by reperfusion of previously hypoperfused cerebral tissues or some other aspect of treatment.

Data from previous studies suggest that hyperglycemia augments ischemic brain injury (27–31). Hyperglycemia results in increased brain lactate concentrations and reduced high-energy phosphate concentrations following an ischemic insult (27,32). During ischemia and reperfusion, hyperglycemia is associated with greater and more prolonged intracellular acidosis (28). Our data correlate well with these findings and suggest that hyperglycemia may result in greater vulnerability of the brain to injury resulting from diminished perfusion.

Although osmotic fluctuations during DKA therapy have been suspected to cause cerebral edema, our data are more consistent with the effects of ischemia and reperfusion. Limited data from other studies suggest that osmotic fluctuations do not result in changes in cerebral high-energy phosphate levels (33). In addition, previous studies by our group have demonstrated high apparent diffusion coefficient (ADC) values measured by magnetic resonance diffusion weighted imaging during DKA treatment in children (3) in contrast to the low ADC values observed in cerebral edema induced by osmotic fluctuations (34–36). These data suggest that declines in osmolality during DKA treatment are unlikely to be the main cause of cerebral injury.

Although clinically apparent cerebral edema develops in only 0.5–1% of DKA episodes in children, recent data suggest that these children may represent only the most severe presentation in a continuum of cerebral injury caused by DKA (4,37). Data from magnetic resonance studies of children undergoing DKA treatment suggest that >50% have measurable cerebral edema (narrowing of the cerebral ventricles) even in the absence of obvious neurological abnormalities (37). Furthermore, recent studies suggest that even apparently uncomplicated DKA may be associated with subtle but permanent neurocognitive deficits in children (38). These data suggest that DKA may cause subtle cerebral injury in many children. Data from the current study suggest that DKA is associated with apparently adverse cerebral metabolic conditions and that these conditions worsen during initial DKA treatment. Whether severe, clinically apparent cerebral edema that develops in a minority of children represents the most extreme manifestation of these metabolic abnormalities or whether additional cerebral insults or metabolic perturbations are necessary to cause clinically apparent cerebral edema is not yet clear. Additional studies will be necessary to resolve this question.

In the current study, treatment with bumetanide, an inhibitor of Na-K-2Cl cotransport, resulted in improvements in metabolic measures during untreated DKA and amelioration of the declines in metabolic measures during initial DKA treatment. These data suggest a protective effect of bumetanide. Previous data from our group have demonstrated that untreated DKA is associated with reduced brain ADC values, suggesting brain cell swelling (1). Bumetanide treatment in these studies resulted in an increase in ADC, suggesting reduced cell swelling. While elucidating the mechanisms underlying this effect of bumetanide will require further investigation, previous studies of the Na-K-Cl cotransporter in healthy and diseased brain provide some clues. The Na-K-Cl cotransporter is known to be present in cerebral microvascular endothelial cells (the BBB), astrocytes, and neurons and to serve a number of functions depending on cell type and prevailing physiological and pathophysiological conditions. These findings have previously been reviewed (39–44). Briefly, in healthy brain, the BBB Na-K-Cl cotransporter (predominantly in the luminal membrane) is thought to participate in secretion of Na, Cl, and water from blood into brain, accounting for up to 30% of brain interstitial fluid generation. During the early hours of ischemic stroke, factors including hypoxia, aglycemia, and vasopressin stimulate activity of the BBB cotransporter, leading to increased secretion of Na, Cl, and water across the intact barrier from blood into brain (42,43,45). Ischemic factors also stimulate astrocyte Na-K-Cl cotransport activity, causing the cells to take up ions and water crossing the BBB and to swell (cytotoxic edema). As ischemia progresses, the endothelial cells themselves begin to swell by a process that is at least partially dependent on Na-K-Cl cotransporter activity. Ischemic stimulation of the cotransporter can also cause swelling of neurons, although there is some debate about the extent of neuronal swelling compared with astrocytes. In addition, increased Na-K-Cl cotransporter activity in GABAergic neurons causes elevation of intracellular [Cl] and thus increased efflux of Cl through GABA-activated Cl channels and depolarization of the cells. Neuronal cotransporter activity is high in immature neurons and appears to contribute to neonatal seizures (41,46,47). In mature brain, the cotransporter may also contribute to seizures occurring after ischemia and reperfusion by increasing intracellular [Cl] and causing hyperexcitability of GABAergic neurons. Previous studies have also shown that elevation of intracellular [Na] stimulates Na/K ATPase activity, consequently increasing ATP consumption as long as ATP is available (48,49); thus, inhibition of Na uptake pathways can decrease ATP consumption (50–53). The observed effects of bumetanide on metabolic parameters in the present study are consistent with the possibilities that *1*) DKA-induced cerebral hypoxia and ischemia stimulates Na-K-Cl cotransporter–medi-

ated Na influx (in BBB, astrocytes, and/or neurons), elevating intracellular [Na] and stimulating Na/K ATPase activity and ATP consumption, and that *2*) bumetanide reduces ATP consumption by reducing cotransporter-mediated Na influx.

Interestingly, although ATP-to-Pi ratio levels were significantly reduced in DKA rats, PCr-to-Pi levels in DKA rats were not significantly different from control values. These data initially appear counterintuitive because declines in PCr-to-Pi ratios caused by cerebral ischemia typically are of greater magnitude than observed declines in ATP-to-Pi ratios (13,14,23,54). Data from human studies of hyperglycemia, however, demonstrate that brain PCr concentrations increase during hyperglycemia (55). A modest increase in ATP concentrations also occurs, but the increase in PCr is greater, resulting in an increase in the PCr-to-ATP ratio. The lack of a detectable difference between DKA rats and controls in PCr-to-Pi ratio in the current study may therefore reflect higher baseline PCr levels in the DKA rats induced by hyperglycemia.

The current study has some limitations. First, under conditions where brain high-energy phosphate metabolism is near normal, Pi levels are commonly near the noise level obtained in our data. This is likely to have caused a relative increase in variability for parameters dependent on Pi (intracellular pH, PCr-to-Pi ratio, and ATP-to-Pi ratio), particularly under control conditions. This variability may have decreased our ability to detect differences of smaller magnitude between groups. In addition, because of the inherent limitations of mechanical ventilation in small animals, we were not always able to precisely adjust the animals' pCO_2 level to that expected for the degree of acidosis. For these reasons, we conducted a subanalysis including the pCO_2 level as a covariate in the model. Inclusion of pCO_2 was not found to improve model fit, suggesting that differences in pCO_2 level between the groups did not have a significant effect on the study outcomes. Finally, although our data suggest a beneficial effect of bumetanide, we investigated only the initial phase of DKA treatment. Whether bumetanide treatment results in decreased neurological injury later in the course of DKA treatment or improved outcomes after recovery from DKA is not yet known.

In summary, our data demonstrate that DKA results in metabolic changes in the brain similar to those occurring in hypoxic and ischemic conditions. Furthermore, initial DKA treatment with insulin and intravenous saline, rather than resulting in improvements in the cerebral metabolic state, results in further deterioration despite recovery of intracellular pH. These data may help to explain the more frequent occurrence of DKA-related cerebral injury during DKA treatment, rather than at the time of presentation. Treatment with bumetanide to inhibit Na-K-2Cl cotransport results in improvements in cerebral metabolic measures, suggesting a protective effect. Our data suggest the need for further investigation of the effects of bumetanide during DKA treatment in children.

ACKNOWLEDGMENTS

This study was supported by National Institutes of Health Grant RO1 NS048610 (to N.G.). This investigation was conducted in part in a facility constructed with support from Research Facilities Improvement Program Grant C06 RR17348-01 from the National Center for Research Resources, National Institutes of Health. Funding for the nuclear magnetic resonance equipment was provided in part by National Science Foundation Grant OSTI 97-24412.

No potential conflicts of interest relevant to this article were reported.

REFERENCES

1. Lam T, Anderson S, Glaser N, O'Donnell M. Bumetanide reduces cerebral edema formation in rats with diabetic ketoacidosis. Diabetes 2005;54:510–516
2. Yuen N, Anderson S, Glaser N, O'Donnell M. Cerebral blood flow and cerebral edema in rats with diabetic ketoacidosis. Diabetes 2008;57:2588–2594
3. Glaser N, Gorges S, Marcin J, Buonocore M, DiCarlo J, Neely E, Barnes P, Bottomly J, Kuppermann N. Mechanism of cerebral edema in children with diabetic ketoacidosis. J Pediatr 2004;145:164–171
4. Glaser N, Marcin J, Wooton-Gorges S, Buonocore M, Rewers A, Strain J, DiCarlo J, Neely E, Barnes P, Kuppermann N. Correlation of clinical and biochemical findings with DKA-related cerebral edema in children using magnetic resonance diffusion weighted imaging. J Pediatr 2008;153:541–546
5. Edge J, Hawkins M, Winter D, Dunger D. The risk and outcome of cerebral oedema developing during diabetic ketoacidosis. Arch Dis Child 2001;85:16–22
6. Glaser N, Barnett P, McCaslin I, Nelson D, Trainor J, Louie J, Kaufman F, Quayle K, Roback M, Malley R, Kuppermann N. Risk factors for cerebral edema in children with diabetic ketoacidosis. N Engl J Med 2001;344:264–269
7. Lawrence S, Cummings E, Gaboury I, Daneman D. Population-based study of incidence and risk factors for cerebral edema in pediatric diabetic ketoacidosis. J Pediatr 2005;146:688–692
8. Duck S, Wyatt D. Factors associated with brain herniation in the treatment of diabetic ketoacidosis. J Pediatr 1988;113:10–14
9. Harris G, Fiordalisi I, Harris W, Mosovich L, Finberg L. Minimizing the risk of brain herniation during treatment of diabetic ketoacidemia: a retrospective and prospective study. J Pediatr 1990;117:22–31
10. Auld K, Ashwal S, Holshouser B, Tomasi L, Perkin R, Ross B, Hinshaw D. Proton magnetic resonance spectroscopy in children with acute central nervous system injury. Pediatr Neurol 1995;12:323–334
11. Holshouser B, Ashwal S, Shu S, Hinshaw D. Proton MR spectroscopy in children with acute brain injury: comparison of short and long echo time acquisitions. J Magn Reson Imaging 2000;11:9–19
12. Kucharczyk J, Moseley M, Kurhanewicz J, Norman D. MRS of ischemic/hypoxic brain disease. Invest Radiol 1989;24:951–954
13. Mitsufuji N, Yoshioka H, Okano S, Nishiki T, Sawada T. A new model of transient cerebral ischemia in neonatal rats. J Cereb Blood Flow Metab 1996;16:237–243
14. Levy RM, Berry I, Moseley M, Weinstein P. Combined magnetic resonance imaging and bihemispheric magnetic resonance spectroscopy in acute experimental focal cerebral ischemia. Acta Radiol Suppl 1986;369:507–511
15. Cady E. Magnetic resonance spectroscopy in neonatal hypoxic-ischaemic insults. Childs Nerv Syst 2001;17:145–149
16. Anderson S, Carr L, Schierling T, Kost G. Are age-related differences in response to myocardial ischemia and cardioplegia pH dependent? Biol Neonate 1994;65:25–35
17. Wooton-Gorges S, Buonocore M, Kuppermann N, Marcin J, DiGirolamo M, Neely E, Barnett P, Glaser N. Detection of cerebral {beta}-hydroxy butyrate, acetoacetate, and lactate on proton MR spectroscopy in children with diabetic ketoacidosis. Am J Neuroradiol 2005;26:1286–1291
18. Robertson J, Shilkofski N. *The Harriet Lane Handbook*. Philadelphia, Elsevier Mosby, 2005, p. 628
19. Keller R, Wolfsdorf J. Isolated growth hormone deficiency after cerebral edema complicating diabetic ketoacidosis. N Engl J Med 1987;316:857–859
20. Lufkin E, Reagan T, Doan D, Yanagihara T. Acute cerebral dysfunction in diabetic ketoacidosis: survival followed by panhypopituitarism. Metabolism 1977;26:363–369
21. Roberts M, Slover R, Chase H. Diabetic ketoacidosis with intracerebral complications. Pediatr Diabetes 2001;2:103–114
22. Cheong J, Cady E, Penrice J, Wyatt J, Cox I, Robertson N. Proton MR spectrsocopy in neonates with perinatal cerebral hypoxic-ischemic injury: metabolite peak-area ratios, relaxation times, and absolute concentrations. Am J Neuroradiol 2006;27:1546–1554
23. Younkin D. Magnetic resonance spectroscopy in hypoxic-ischemic encephalopathy. Clin Invest Med 1993;16:115–121
24. Moseley M, Cohen Y, Mintorovich J, Chileuitt L, Shimizu H, Kucharczyk J, Wendland MF, Weinstein PR. Early detection of regional cerebral ischemia

in cats: comparison of diffusion- and T2-weighted MRI and spectroscopy. Magn Reson Med 1990;14:330–346
25. Malisza K, Kozlowski P, Peeling J. A review of in vivo 1H magnetic resonance spectroscopy of cerebral ischemia in rats. Biochem Cell Biol 1998;76:487–496
26. Levine S, Helpern J, Welch K, AM VL, Sawaya K, Brown E, Ramadan N, Deveshwar R, Ordidge R. Human focal cerebral ischemia: evaluation of brain pH and energy metabolism with P-31 NMR spectroscopy. Radiology 1992;185:537–544
27. Chew W, Kucharczyk J, Moseley M, Derugin N, Norman D. Hyperglycemia augments ischemic brain injury: in vivo MR imaging/spectroscopic study with nicardipine in cats with occluded middle cerebral arteries. Am J Neuroradiol 1991;12:603–609
28. Dempsey R, Baskaya M, Combs D, Donaldson D, Rao A. Effect of hyperglycemia on reperfusion-associated recovery of intracellular pH and high energy phosphates after transient cerebral ischemia in gerbils. Neurol Res 1996;18:546–552
29. Alvarez-Sabin J, Morrison R, Ribo M, Arenillas J, Montaner J, Huertas R, Santamarina E, Rubiera M. Impact of admission hyperglycemia on stroke outcome after thrombolysis: risk stratification in relation to time to reperfusion. Stroke 2004;35:2493–2498
30. Ennis S, Keep R. Effect of sustained-mild and transient-severe hyperglycemia on ischemia-induced blood-brain barrier opening. J Cereb Blood Flow Metab 2007;27:1573–1582
31. Martin A, Rojas S, Chamorro A, Falcon C, Bargallo N, Planas A. Why does acute hyperglycemia worsen the outcome of transient focal cerebral ischemia? Role of corticosteroids, inflammation, and protein O-glycosylation. Stroke 2006;37:1288–1295
32. Levine S, Welch K, Helpern J, Chopp M, Bruce R, Selwa J, Smith M. Prolonged deterioration of ischemia brain energy metabolism and acidosis associated with hyperglycemia: human cerebral infarction studied by serial 31P NMR spectroscopy. Ann Neurol 1988;23:416–418
33. Adler S, Simplaceanu V. Effect of acute hyponatremia on rat brain pH and rat brain buffering. Am J Physiol 1989;256:F113–F119
34. Righini A, Ramenghi L, Zirpoli S, Mosca F, Triulzi F. Brain apparent diffusion coefficient decrease during correction of severe hypernatremic dehydration. Am J Neuroradiol 2005;26:1690–1694
35. Sevick R, Kanda F, Mintorovitch J, Arieff A, Kucharczyk J, Tsuruda J, Norman D, Moseley M. Cytotoxic brain edema: assessment with diffusion-weighted MR imaging. Radiology 1992;185:687–690
36. Vajda Z, Pedersen M, Doczi T, Sulyok E, Stodkilde-Jorgensen H, Frokiaer J, Nielsen S. Effects of centrally administered arginine vasopressin and atrial natriuretic peptide on the development of brain edema in hyponatremic rats. Neurosurgery 2001;49:697–705
37. Glaser N, Wooton-Gorges S, Buonocore M, Marcin J, Rewers A, Strain J, DiCarlo J, Neely E, Barnes P, Kuppermann N. Frequency of sub-clinical cerebral edema in children with diabetic ketoacidosis. Pediatr Diab 2006;7:75–80
38. Ghetti S, Lee J, Sims CE, Demaster D, Glaser N. Diabetic ketoacidosis and memory dysfunction in children with type 1 diabetes. J Pediatr 2010;156:109–114
39. Foroutan S, Brillault J, Forbush B, O'Donnell M. Moderate to severe ischemic conditions increase activity and phosphorylation of the cerebral microvascular endothelial cell Na-K-Cl cotransporter. Am J Physiol Cell Physiol 2005;289:C1492–C1501
40. Blaesse P, Airaksinen M, Rivera C, Kaila K. Cation-chloride cotransporters and neuronal function. Neuron 2009;61:820–836
41. Kahle K, Staley K, Nahed B, Gamba G, Hebert S, Liption R, Mount D. Roles of the cation-chloride cotransporters in neurological disease. Nat Clin Pract Neurol 2008;4:490–503
42. O'Donnell M, Duong S, Suvatne S, Foroutan S, Johnson D. Arginine vasopressin stimulation of cerebral microvascular endothelial cell Na-K-Cl cotransport activity is V1 receptor- and [Ca]-dependent. Am J Physiol Cell Physiol 2005;289:C283–C292
43. O'Donnell M, Tran L, Lam T, Liu X, Anderson S. Bumetanide inhibition of the blood-brain barrier Na-K-Cl cotransporter reduces edema formation in the rat middle cerebral artery occlusion model of stroke. J Cereb Blood Flow Metab 2004;24:1046–1056
44. Pedersen S, O'Donnell M, Anderson S, Cala P. Physiology and pathophysiology of Na^+/H^+ exchange and $Na^+/K^+/2Cl^-$ cotransporter in the heart, brain, and blood. Am J Physiol Regul Integr Comp Physiol 2006;291:R1–R25
45. Brillault J, Lam T, Rutkowsky J, Foroutan S, O'Donnell M. Hypoxia effects on cell volume and ion uptake of cerebral microvascular endothelial cells. Am J Physiol 2008;294:C88–C96
46. Dzhala V, Talos D, Sdrulla D, Brumback A, Mathwes G, Benke T, Delpire E, Jensen F, Staley K. NKCC1 transporter facilitates seizures in the developing brain. Nat Med 2005;11:1205–1213
47. Kahle K, Barnett S, Sassower K, Saley K. Decreased seizure activity in a human neonate treated with bumetanide, an inhibitor of the Na+-K+-2Cl-cotransporter NKCC1. J Child Neurol 2009;24:572–576
48. Anderson S, Dickinson C, Liu H, Cala P. Effects of Na-K-Cl cotransport inhibition on myocardial Na and Ca during ischemia and reperfusion. Am J Physiol 1996;270:C608–C618
49. Erecińska M, Nelson D, Dagani F, Deas J, Silver I. Relations between intracellular ions and energy metabolism under acidotic conditions: a study with nigericin in synaptosomes, neurons, and C6 glioma cells. J Neurochem 1993;61:1356–1368
50. Matsuda T, Shimizu I, Murata Y, Baba A. Glucose and oxygen deprivation induces a Ca(2+)-mediated decrease in (Na(+)+K+)-ATPase activity in rat brain slices. Brain Res 1992;576:263–270
51. Pond B, Galeffi F, Aheren R, Schwartz-Bloom R. Chloride transport inhibitors influence recovery from oxygen-glucose deprivation-induced cellular injury in adult hippocampus. Neuropharmacology 2004;47:253–262
52. Ramasamy RJ, Payne A, Whang J, Bergmann S, Schaefer S. Protection of ischemic myocardium in diabetics by inhibition of electroneutral Na+-K+-2Cl- cotransporter. Am J Physiol Heart Circ Physiol 2001;281:H515–H522
53. Hochachka P, Buck L, Doll C, Land S. Unifying theory of hypoxia tolerance: molecular/metabolic defense and rescue mechanisms for surviving oxygen lack. Proc Natl Acad Sci 1996;93:9493–9498
54. Germano I, Pitts L, Berry I, DeArmond S. High energy phosphate metabolismin experimental permanent focal cerebral ischemia: an in vivo 31P magnetic resonance spectroscopy study. J Cereb Blood Flow Metab 1987;8:24–31
55. Oltmanns K, Melchert U, Scholand-Engler H, Howitz M, Schultes B, Schweiger U, Hohagen F, Born J, Peters A, Pellerin L. Differential energetic response of brain vs. skeletal muscle upon glycemic variations in humans. Am J Physiol Regul Intergr Comp Physiol 2007;294:R12–R16